

Purification of Active TFIID from *Saccharomyces cerevisiae*

EXTENSIVE PROMOTER CONTACTS AND CO-ACTIVATOR FUNCTION*

Received for publication, August 26, 2004, and in revised form, September 20, 2004
Published, JBC Papers in Press, September 22, 2004, DOI 10.1074/jbc.M409849200

Roy Auty^{‡§}, Hanno Steen[¶], Lawrence C. Myers^{||}, Jim Persinger^{**}, Blaine Bartholomew^{**},
Steven P. Gygi[¶], and Stephen Buratowski^{‡ ††}

From the [‡]Department of Biological Chemistry and Molecular Pharmacology and the [¶]Department of Cell Biology, Harvard Medical School, Boston, Massachusetts 02115, the ^{||}Department of Biochemistry, Dartmouth Medical School, Hanover, New Hampshire 03755, and the ^{**}Department of Biochemistry and Molecular Biology, Southern Illinois University, Carbondale, Illinois 62901

The basal transcription factor TFIID is composed of the TATA-binding protein (TBP) and 14 TBP-associated factors (TAFs). Although TBP alone binds to the TATA box of DNA and supports basal transcription, the TAFs have essential functions that remain poorly defined. In order to study its properties, TFIID was purified from *Saccharomyces cerevisiae* using a newly developed affinity tag. Analysis of the final elution by mass spectrometry confirms the presence of all the known TAFs and TBP, as well as Rsp5, Bul1, Ubp3, Bre5, Cka1, and Cka2. Both Taf1 and Taf5 are ubiquitinated, and the ubiquitination pattern of TFIID changes when *BUL1* or *BRE5* is deleted. Purified TFIID binds specifically to promoter DNA in a manner stabilized by TFIIA, and these complexes can be analyzed by native gel electrophoresis. Phenanthroline-copper footprinting and photoaffinity cross-linking indicate that TFIID makes extensive contacts upstream and downstream of the TATA box. TFIID supports basal transcription and activated transcription, both of which are enhanced by TFIIA.

TFIID is a large, multisubunit complex that is essential for transcription by RNA polymerase II. It consists of the TATA-binding protein (TBP)¹ and at least 14 TBP-associated factors (TAFs) (1). Although the sizes of these TAFs differ by organism, conserved domains reflect that these proteins have been conserved over the eukaryotic evolution (2). TBP is necessary and sufficient for binding to the TATA box sequence, although this binding is stabilized by the addition of TFIIA and TFIIB (3). Yeast TFIIA is a complex of two proteins that binds TBP and makes contacts with the DNA immediately upstream of the TATA box (4–6). Human TFIID also binds DNA in a TATA-

specific fashion but makes additional downstream contacts that may allow binding to promoters lacking a TATA element (7). In human and *Drosophila melanogaster* promoters, a significant element is the initiator region about 25 bp downstream of the TATA box. The two largest TAFs, hTaf1 and hTaf2, may contact the initiator region directly (8). Within *Drosophila* TFIID, it has been proposed that some of the histone-like TAFs interact with a downstream promoter element situated at approximately +30 relative to the transcription start site (9). In yeast, the TATA box is usually situated 50–90 bp upstream of the transcription start sites, but no clear consensus sequences have emerged for a downstream promoter element or initiator region.

Although the yeast system has been extremely useful for studying the genetics of TAFs, there have been comparatively few biochemical studies of yeast TFIID. Immunoaffinity purification of the complex has been successful, but yields are relatively low, and the procedure requires large amounts of antibodies. Nonetheless, analysis of immunopurified yeast TFIID by mass spectrometry led to the confirmation of TFIID composition and estimates of subunit stoichiometry (1). Another study using DNase I protection found that γ TFIID binding was centered on the TATA box but made additional contacts up to 45 bp downstream and 25 bp upstream (10). These additional contacts were not seen with TBP alone and were dependent upon the presence of TFIIA. Two other studies have used antibodies to map subunits within the TFIID complex (11, 12). However, the production of larger amounts of active TFIID would greatly facilitate studies of interactions with DNA and its role in the control of transcription.

This paper describes the development of a multipart affinity tag that can be used to purify protein complexes. This tag was used to purify significant amounts of native yeast TFIID. The purified TFIID binds to DNA in a TATA-specific fashion. In combination with TFIIA, TFIID makes extended contacts with the DNA upstream and downstream of the TATA box. Dissection of these contacts indicates the orientation and provides additional structural information about TFIID. The purified TFIID supports basal transcription *in vitro* and can also mediate activated transcription in the absence of Mediator. In addition to the expected TAFs and TBP, mass spectrometry of the TFIID fraction identified several possible TFIID-associated proteins, including proteins that may be important for the regulation of transcription by ubiquitination.

MATERIALS AND METHODS

Construction of the HCHH-Taf13 Expression Construct—pRS315-HCHH was constructed in several steps. PCR was used to amplify the calmodulin binding domain and tobacco etch virus (TEV) protease site from pBS1479 (13). The upstream primer was designed to add six

* This work was supported in part by National Institutes of Health Grants GM62483 (to L. C. M.) and GM46498 (to S. B.). The costs of publication of this article were defrayed in part by the payment of page charges. This article must therefore be hereby marked "advertisement" in accordance with 18 U.S.C. Section 1734 solely to indicate this fact.

§ Supported by a Howard Hughes Medical Institute predoctoral fellowship.

†† Scholar of the Leukemia and Lymphoma Society. To whom correspondence should be addressed: Dept. of Biological Chemistry and Molecular Pharmacology, Harvard Medical School, 240 Longwood Ave., Boston, MA 02115. Tel.: 617-432-0696; Fax: 617-738-0516; E-mail: steveb@hms.harvard.edu.

¹ The abbreviations used are: TBP, TATA-binding protein; CBP, calmodulin-binding peptide; TEV, tobacco etch virus; TAFs, TBP-associated factors; HA, hemagglutinin; BisTris, 2-[bis(2-hydroxyethyl)amino]-2-(hydroxymethyl)propane-1,3-diol; MOPS, 4-morpholinepropanesulfonic acid; EMSA, electrophoretic mobility shift assays; CK2, casein kinase II; OP-Cu, copper-phenanthroline; AdMLP, Adenovirus major late promoter.

additional histidine residues. This cassette was then ligated between a 458-bp fragment of the *TFA1* promoter and a triple HA epitope tag. This combined module was subcloned from pUC19 into pRS315. The *TAF13* coding region was inserted in-frame into a BglII site just downstream of the HA tags. Finally, an additional fragment encoding eight histidine residues was ligated into an NheI site to generate pRS315-HCHH-TAF13. The sequence of this plasmid is available upon request. YSB721 has a genotype of *MATa ura3-52 leu2::PET56 trp1 his3Δ200 ade2-1 taf13Δ::HIS3* (pRS316-TAF13). YSB867 was constructed by plasmid shuffling to replace pRS316-TAF13 with pRS315-HCHH-TAF13.

TFIID Purification—Twelve liters of 1.5× YPD supplemented with adenine and tryptophan were inoculated with 20 ml of a saturated culture of YSB867. Cells were grown in a fermentor for 40 h to an optical density at 590 nm, yielding 240 g of cells. 120 grams of frozen cells were ground with a pestle and mortar in the presence of liquid nitrogen. Cells were then thawed and resuspended in 90 ml of KBF1 lysis buffer (50 mM HEPES-KOH (pH 7.6), 10% glycerol, 0.3% Nonidet P-40, 2 mM MgSO₄, 2 mM CaCl₂, 150 mM potassium acetate (KOAc), 2.5 mM β-mercaptoethanol, 10 μg/ml each of aprotinin, leupeptin, and pepstatin A, 1 mM phenylmethylsulfonyl fluoride). An equal volume of 425–600-μm glass beads was added, and cells were further lysed in a Bead-Beater (Bio-spec products) using 15 cycles of 20 s on, 100 s off. The supernatant was decanted, and any remaining beads and cell debris were removed by centrifugation at 6000 × *g* for 6 min in an SS-34 rotor. The KOAc concentration of the supernatant was adjusted to 650 mM. The sample was incubated at 4 °C for 30 min to allow extraction of nuclei, and the lysate was then centrifuged at 100,000 × *g* in a Beckman 45Ti rotor for 60 min. The clarified supernatant was diluted by a factor of 2 with KBF2 buffer (KBF1 lacking KOAc) and rotated overnight with 2.4 ml of Calmodulin-Sepharose (Amersham Biosciences). The slurry was poured into four short columns, washed with 5 column volumes of KBF1, and eluted in 7.2 ml of KBF3 elution buffer (25 mM HEPES-KOH (pH 7.6), 10% glycerol, 0.3% Nonidet P-40, 2 mM MgSO₄, 5 mM EGTA, 350 mM KOAc, 2.5 mM mercaptoethanol). The elution fraction was diluted by a factor of 5 with KBF2 and loaded onto a Hi-S cation exchange column (Amersham Biosciences). The column was developed by gradient elution in 6.5 ml from 75 to 675 mM KOAc. Fractions that contained TFIID were identified by SDS-PAGE and immunoblotting for TBP and multiple TAFs. 1.5 ml of the fractions eluting from 400 to 550 mM KOAc were pooled and incubated with 60 μl of TALON resin (Clontech) for 3 h and washed three times with 1 ml of KBF7-15 (15 mM imidazole, 25 mM HEPES-KOH (pH 7.6), 10% glycerol, 0.025% Nonidet P-40, 2 mM MgSO₄). The slurry was poured into a column and eluted with 4 elutions of 60 μl of KBF7-400 (the same buffer with 400 mM imidazole). The final eluate was dialyzed against KBF8 (25 mM HEPES-KOH (pH 7.6), 10% glycerol, 150 mM KOAc, 0.5 mM EDTA, 0.5 mM dithiothreitol, 0.5 mM MgOAc) using dialysis membrane with a nominal molecular weight cut-off of 6–8000 (Spectrapor). The sample was concentrated by further dialysis against KBF8 containing 30% PEG-8000 until the volume was ~120 μl. The dialysis steps were required to remove imidazole, leading to improved long term storage and reduced background in DNA binding experiments. Final protein concentration was determined by using a Bradford-style dye-binding assay (Bio-Rad). TFIID fractions were analyzed by SDS-PAGE stained with colloidal Coomassie Blue (Sigma B2025) and by immunoblotting for TFIID components and ubiquitin (Affiniti UG9510).

Mass Spectrometry—Approximately 15 μg of TFIID were analyzed by SDS-PAGE using a MOPS-NuPAGE 4–12% BisTris gradient gel. After staining with colloidal Coomassie Blue, 30 gel slices containing visible bands were excised, reduced, alkylated, and digested overnight with trypsin prior to analysis by mass spectrometry. Peptide digests were analyzed by liquid chromatography/mass spectrometry. The liquid chromatography system consisted of an in-house prepared microscale capillary reversed phase column (outer diameter 360 μm, inner diameter 100 μm) packed with 5 μm/200 Å Magic C18 beads (Michrom BioResources) and an Agilent 1100 high pressure liquid chromatography pump. The mass spectrometer was a QSTAR Pulsar I (Applied Biosystems/MDS-Sciex). The protein digest was loaded onto the column using either a pressure cell or a Famos autosampler (LC Packings). The data were searched against the yeast protein data base (NCBI) using the ProID software package (Applied Biosystems). In addition, several unseparated protein complex samples were digested in solution with trypsin and then analyzed by liquid chromatography/mass spectrometry as above. Although polyethylene glycol from these samples complicated analysis, peptides identified matched those proteins identified by gel electrophoresis.

Electrophoretic Mobility Shift Assay—DNA probes were excised from plasmids with restriction enzymes and labeled on one strand by filling

in with Klenow fragment and the appropriate combination of radioactive and unlabeled dNTPs. Adenovirus major late promoter (AdMLP) sequences were from pUC-MLTATAwt and pUC-MLTATAmut2 (14). Probes containing about 115 bp of *ADH1* or *ADH2* promoter sequences were generated by annealing long oligonucleotides, extending with a single round of PCR, and cloning these fragments into pUC19ΔH3. Four point mutations were introduced to disrupt cryptic TATA boxes in each promoter (pUC-Adh1Pro and pUC-Adh2Pro). *ADH1* and *ADH2* promoters with mutated TATA boxes were generated using identical oligonucleotides except for the TATAA sequence that was changed to GCGTC (pUC-Adh1MutPro) and GGGCG (pUC-Adh2MutPro), respectively. All sequences are available upon request. Binding reactions were 10 μl and contained ~2 μg of TFIID, 100 mM NaCl, 2 mM MgOAc, 1 mM EGTA, 2 mM dithiothreitol, 10 μg of bovine serum albumin, 5% glycerol, 0.3 μg of dGdC, and 10,000 cpm end-labeled probe. After 30 min of incubation at room temperature, reactions were resolved on 1.6% agarose gels in 1× TGE (25 mM Tris base, 190 mM glycine, 1 mM EDTA) with 2 mM MgOAc and/or 1% glycerol. The 4-mm thick gels were run at 7.5 V/cm for 50 min at room temperature. Gels were dried and exposed to film or a PhosphorImager plate for 40 min to overnight. Some reactions also included 0.5 μl of 2 μM recombinant TFIIA (a gift from Song Tan, Pennsylvania State University), 0.5 μl of 2 μM recombinant TBP, and/or 0.5 μl of 2 μM recombinant TFIIB.

Phenanthroline-Copper Footprinting—EMSA was performed as above with some minor changes. To scale up the reaction, ~4 μg of TFIID or 50 ng of TBP were used in combination with 100 ng of TFIIA and 25,000 cpm of probe. Low melting point agarose was used. Instead of drying the gel, copper-phenanthroline chemical footprinting was performed *in gel* (15) for 10 min prior to quenching and overnight exposure of the wet gel to film. Gel slices containing TBP or TFIID-bound DNA complex and unbound DNA were excised and melted, phenol-extracted twice, chloroform-extracted, ethanol-precipitated, and then counted using a scintillation counter. The samples were normalized to equalize radioactive counts, denatured, and resolved on an 8% polyacrylamide sequencing gel (1× TBE, 8 M urea). These gels were fixed by soaking in 10% methanol, 10% acetic acid, dried, and exposed to a PhosphorImager plate overnight. Results were analyzed using ImageJ (National Institutes of Health).

DNA Photoaffinity Labeling—Nine different probes were constructed, each containing an 5-[N-(4-azidobenzoyl)-3-aminooethyl]-dUTP residue followed by a ³²P-radiolabeled nucleotide (16, 17). Cross-linker and label were incorporated at a specific sites on the sense strand of 100 bp of *ADH1* promoter sequence. Two point mutations were introduced in *ADH1* to increase the number of sites for cross-linking. Following synthesis, probes were normalized for total counts. Binding reactions were prepared as above for EMSA. After incubation in the dark, cross-linking was activated by illumination with a long wavelength UV light for 4 min. DNA was nicked with DNase I (Ambion) and digested with S1 nuclease (U. S. Biochemical Corp.) prior to analyzing cross-linked proteins on a 4–20% gradient polyacrylamide gel for SDS-PAGE. The gels were dried and exposed to a PhosphorImager plate overnight. The PhosphorImager was quantified, with background correction for each lane and normalization of each TAF relative to an unchanging band.

In Vitro Transcription Reactions—Yeast TFIIB, TFIIE, TFIIF, Mediator, and RNA polymerase II were purified as described (18). Yeast TBP (14), full-length TFIIA (6), and TFIIF (19) were also purified for use in a specific transcription assay (20). Briefly, transcription reactions with purified factors were incubated at 23 °C for 60 min with 100 ng of template plasmids pS(GCN4)²CG⁻ and pJJ470 before being stopped by 6-fold dilution with stop solution (10 mM Tris-Cl (pH 7.5), 0.3 M NaCl, 5 mM EDTA, 0.1 mg/ml glycogen, and 12.5 units/ml ribonuclease T1). 10% SDS and proteinase K were added to remove protein prior to ethanol precipitation, denaturation, and analysis on a 7% acrylamide, 7 M urea TBE gel.

RESULTS

Purification of TFIID—To facilitate purification of native TFIID, we designed a new affinity tag (Fig. 1A), which we designated HCHH. Although it shares some features with the TAP tag (13), it is smaller (at 118 residues) and does not absolutely require protease cleavage for elution. The HCHH tag consists of an N-terminal 6-histidine tag followed by the calmodulin-binding peptide (CBP). This is followed by another stretch of 8 histidine residues with 10 residue linkers on either side. These elements are separated from a triple-HA epitope tag by a cleavage site for the TEV protease. The cleavage site

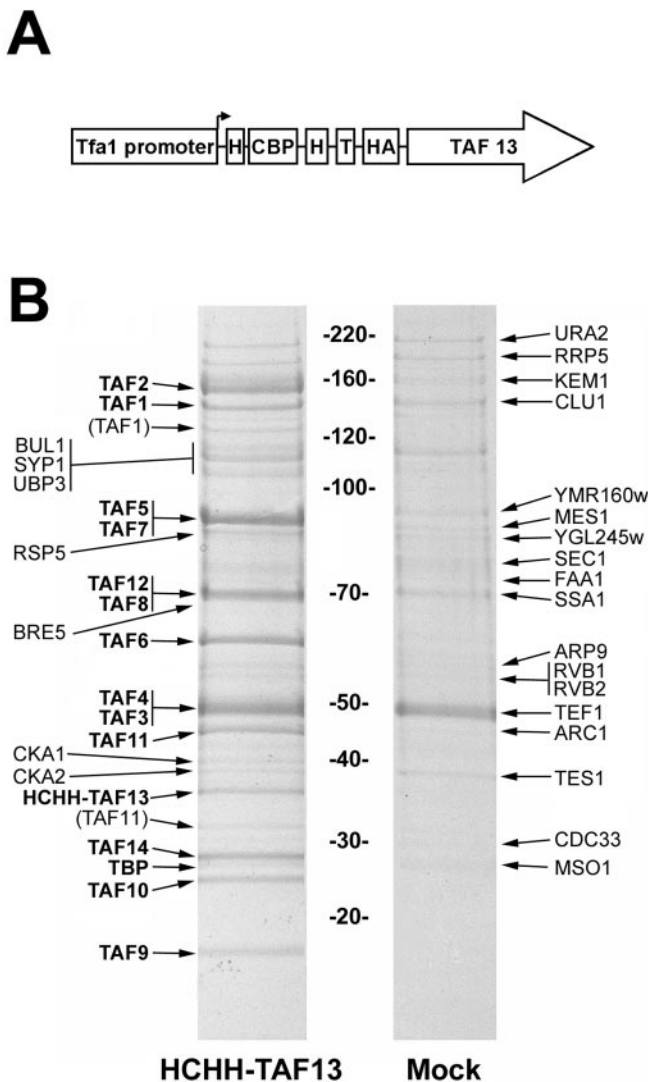


FIG. 1. Purification of yeast TFIID using HCHH-tagged Taf13. A, schematic diagram of the tagged expression cassette. The cassette contains (from left to right) the *TFA1* promoter (small black arrow designates the transcription start site), 6 histidine residues (H), a calmodulin-binding peptide (CBP), 8 histidine residues (H), and three hemagglutinin tags (HA). The tag is cloned in-frame with the *TAF13* open reading frame. B, Coomassie-stained polyacrylamide gel of the purified TFIID. Extracts from tagged strain YSB867 (*HCHH-Taf13*) and the untagged parent strain YSB721 were chromatographed over three columns as described under "Materials and Methods." The final fraction was electrophoresed on a 4–12% gradient gel. Band assignments were made based on mass spectrometric analysis of 30 individual gel slices from the HCHH-Taf13 preparation lane. Probable contaminants that were present in both lanes are annotated on the right. Bul1, Syp1, and Ubp3 are shown together because the three designated bands were cut out and analyzed together. Bands designated in parentheses are either breakdown products of the larger, full-length proteins or otherwise modified in a way that causes altered mobility.

may be used to separate the protein from the final affinity column or simply to remove the tag after it is no longer necessary. The HCHH tag was cloned into a low copy yeast shuttle vector downstream of the constitutive *TFA1* promoter. For purification of TFIID, the open reading frame of the TFIID-specific *TAF13* was cloned in-frame C-terminal to the HCHH tag. The expression plasmid was shuffled into a *taf13Δ* strain to create YSB867. No obvious growth differences were observed between the tagged strain and its parent, suggesting that the HCHH tag does not interfere with Taf13 function.

Conditions for lysis of yeast cells and protein extraction were optimized for maximum levels of TFIID in the soluble fraction.

The first purification step was chromatography on Calmodulin-Sepharose, from which proteins were eluted with a combination of EGTA and moderate salt. Because the EGTA was not compatible with immobilized metal affinity chromatography, the calmodulin eluate was run over a strong cation exchange column (Hi-S). Fractions were analyzed by immunoblotting, and those containing the HA epitope were pooled and bound to cobalt-nitrilotriacetic acid resin. From 120 g of yeast, ~100 μ g of the TFIID fraction were obtained. Assuming 5000 molecules of TFIID per cell (21) and 2.5×10^{11} cells per purification, 100 μ g of total protein means the procedure approaches a recovery of 4%. Quantitative immunoblotting yields an estimate of purity of about 30–50% so the final recovery is probably closer to 1–2%.

Gel filtration chromatography and glycerol gradient analyses (not shown) confirmed that the purification yields a single complex with an apparent molecular mass of 700 kDa. Further purification by anion exchange chromatography also produced a single elution peak (data not shown). Quantitative immunoblotting of a typical purification gave a final concentration of ~200 nM for TBP and ~400 nM for Taf13, the tagged "entry point" for the purification (data not shown). Therefore, at least 50% of the recovered TAF complexes contain TBP.

Identification of TFIID-associated Proteins—Proteins within the purified TFIID fractions were analyzed by mass spectrometry. The samples were analyzed both as whole complex digested in solution and as single bands after separation by SDS-PAGE and in gel digestion. Thirty individual band slices were excised from a gel similar to the one shown in the 1st lane of Fig. 1B for analysis. A parallel purification from an untagged strain was carried out to identify nonspecifically associated proteins (Fig. 1B, 2nd lane). All 14 TAFs and TBP were identified in the TFIID preparation, both in whole sample and individual band analyses. Multiple peptides for each TAF were observed, with sequence coverage ranging from 35 to 65%.

Peptides from eight of the TAFs appeared in more than one gel band. In most cases this was because of cross-contamination of the excised gel slices and/or partial proteolysis. One prominent example of the latter was the identification of 37 peptides within one band of about 120 kDa, corresponding to a fragment of Taf1 that may be missing up to 198 residues from the N terminus. Another likely possibility is that some TAFs undergo post-translational modification. No phosphorylated peptides were identified by mass spectrometry. However, methylation on Taf5 was observed.² In cases where a TAF appeared in multiple bands, the band that clearly produced more peptides and sequence coverage than the others was the one annotated in Fig. 1B.

In addition to the previously known TFIID subunits, several other proteins were identified in the purified fraction. Most of these correspond to bands in the mock-purified lane of Fig. 1B. For example, bands identified as Mes1, YGL245w, and Arc1 were seen in both lanes. These proteins are known to form a complex that binds tRNA (22). In addition, several abundant proteins that are often found as contaminants were identified. These include heat shock proteins, the translation elongation factor Tef1, and the Kem1 protein (23).

There are some other proteins in the TAF13-HCHH purified lane that do not appear to be in the mock-purified lane (Fig. 1B). These included Cka1 and Cka2, components of the kinase CK2. Several of the other candidate TFIID-interacting proteins have roles in ubiquitination. The ubiquitin ligase Rsp5 and its heterodimer partner Bul1 were both identified with about 9% sequence coverage. Also, the ubiquitin protease Ubp3 and its

² R. Auty and S. Buratowski, manuscript in preparation.

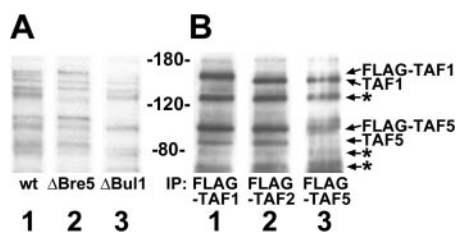


FIG. 2. Taf1 and Taf5 are ubiquitinated. A, TFIID was purified using HCHH-TAF13 from a wild-type strain (lane 1), a *BRE5* deletion strain (lane 2), and a *BUL1* deletion strain (lane 3). TFIID preparations were run on 10% polyacrylamide gels, transferred to nitrocellulose, and immunoblotted with anti-ubiquitin antibody. B, the indicated FLAG-tagged TAFs were immunoprecipitated (IP) using anti-FLAG M2-agarose (Sigma) and eluted with glycine at pH 3.0. Immunoprecipitates were analyzed for ubiquitinated proteins by immunoblotting as in A. Lane 1 shows a FLAG-Taf1 immunoprecipitation; lane 2 shows FLAG-Taf2; and lane 3 shows FLAG-Taf5. Asterisks denote unidentified bands that did not change in the different preparations. Note the mobility shifts associated with the FLAG tags on Taf1 and Taf5. Because no shifts of ubiquitinated bands are seen with tagged Taf2, we conclude that it is not ubiquitinated.

targeting subunit Bre5 were also identified, with 15 and 48% sequence coverage, respectively. Although *RSP5* is required for viability, the genes encoding Ubp3 and the adaptor proteins Bre5 and Bul1 can be deleted with no ill effects. The HCHH-tagged Taf13 was expressed in yeast strains deleted for either *BRE5* or *BUL1*. Purified TFIID complexes from these strains and a wild-type strain were analyzed by immunoblotting with anti-ubiquitin antibody (Fig. 2A). Multiple ubiquitinated proteins are observed in wild-type extracts (Fig. 2A, lane 1), although some groups of bands may represent multiple ubiquitinations of the same protein. Deletion of the deconjugase adaptor Bre5 results in enrichment of higher molecular weight species (Fig. 2A, lane 2). Conversely, deletion of the ligase adaptor Bul1 strongly reduces levels of several ubiquitinated species that co-purify with HCHH-TAF13. To test whether any of these ubiquitinated proteins are TAFs, TFIID was immunoprecipitated from FLAG-tagged Taf1, Taf2, and Taf5 strains. The precipitates were analyzed by immunoblotting with anti-FLAG antibody to confirm that equal amounts of TFIID were immunoprecipitated (data not shown) and with anti-ubiquitin antibody (Fig. 2B). The mobility shifts provided by the FLAG tag indicates clearly that Taf1 (Fig. 2B, lane 1) and Taf5 (Fig. 2B, lane 3) are ubiquitinated proteins. Furthermore, these proteins migrate similarly to the ubiquitinated proteins in the HCHH-Taf13 purification that are affected by deletions in Bre5 and Bul1. Although tagged Taf2 is present in Fig. 2B, lane 2, it is apparently not ubiquitinated and thus serves as a negative control.

Although we and others have found bromodomain factor 1 (Bdf1) associated with TFIID in direct binding experiments (1, 24) and as part of the pre-initiation complex (25), we did not detect Bdf1 in our TFIID preparation by mass spectrometry. This was not too surprising because we have found that Bdf1 association with TFIID is very sensitive to moderate salt levels.³ We have also recently found that Bdf1 binds to and is phosphorylated by CK2 (26), which is present in our TFIID preparation. When we used a more sensitive phosphorylation assay, a small amount of Bdf1 was observed (data not shown). This is in agreement with Sanders *et al.* (1), who also detected substoichiometric amounts of Bdf1 in their TFIID preparation by mass spectrometry.

TFIID Binding to DNA Promoter Sequences—To test the ability of our purified TFIID to bind to typical yeast and adenoviral promoters, EMSAs were performed. Experiments us-

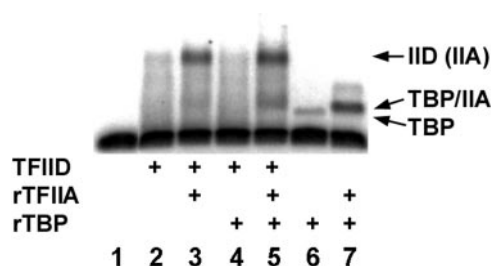


FIG. 3. Native gel electrophoresis of TFIID, TFIIA, and DNA. TBP or TFIID binding to a ³²P-labeled AdMLP probe was assessed by separating bound complex from free probe in a 1.6% agarose gel containing 2 mM Mg²⁺. TFIIA was added as indicated. The complexes formed in the presence and absence of TFIIA are designated on the right.

ing native acrylamide gels were unsuccessful, but agarose gels allowed detection of the large TFIID-DNA complex (Fig. 3). TFIID alone can retard a DNA fragment containing the AdMLP. The TFIID-DNA complex migrated much more slowly than the TBP-DNA complex. However, TFIID complexes were smeared in the gel, presumably due to dissociation during electrophoresis (Fig. 3, lane 2). Fig. 3, lane 3, shows that equimolar amounts of TFIIA strongly stabilized TFIID binding in this assay. TBP binding was also stabilized by TFIIA (Fig. 3, compare lanes 6 and 7). TFIIA by itself showed no binding to the probe (data not shown). The addition of extra TBP did not significantly increase the amount of TFIID binding (Fig. 3, compare lanes 2 and 4), suggesting that most of the purified TAF complexes contain TBP. Similar results were obtained when yeast *ADH1* or *ADH2* promoters were used (data not shown and see below).

To test whether TFIID binding was dependent upon a functional TATA element, EMSA competition experiments were performed by adding increasing amounts of unlabeled AdMLP DNA fragments. Although a fragment containing a wild-type TATAA box was able to compete for TFIID, a similar fragment in which the TATAA sequence was mutated to GCGTC competed less efficiently (data not shown). Although competition by the mutant was much reduced, it was not completely eliminated. This suggests that additional contacts may be made on DNA apart from the TATA box. When the mutant AdMLP fragment was labeled, low levels of TFIID binding were still observed that were not seen with TBP alone (data not shown).

Extensive Contacts between TFIID and Promoter Sequences—If TFIID makes additional contacts with promoter sequences outside of the TATA box, these should be observable using DNA footprinting techniques. Indeed, DNase I protection experiments suggest that mammalian TFIID makes extensive contacts with DNA downstream of the TATA element to at least 35 bp downstream of the initiation site (27, 28). Increased DNase I sensitivities up to 20 bp upstream of the TATA element have also been reported (see also Ref. 7). More recently, yeast TFIID was shown to alter DNase I digestions patterns as far as 25 bp upstream and 45 bp downstream of the TATA element (10).

To confirm and extend these earlier findings, we used copper-phenanthroline (OP-Cu) chemical footprinting. OP-Cu reacts directly with deoxyribose so that digestion can be obtained with single base resolution (29). This reagent is well suited for studying the TATAA box because A-T-rich regions tend to be more susceptible (15). EMSA was performed to isolate TBP-TFIIA and TFIID-TFIIA complexes bound to the *Saccharomyces cerevisiae ADH1* or *ADH2* promoters. Chemical cleavage was carried out in the native gel. Following recovery and purification, the cleaved DNAs were analyzed on a sequencing gel (Fig. 4). Fig. 4, lanes 1–3, shows the sense strand for each

³ C. Sawa and S. Buratowski, unpublished data.

promoter, and Fig. 4, lanes 4–6, show the antisense strand.

Unbound DNA (Fig. 4, lanes 3 and 6) was cleaved throughout, but the regions of the TATA elements (Fig. 4, A and B, arrows) were particularly susceptible to OP-Cu cutting. TBP/TFIIA (Fig. 4, A and B, lanes 1 and 4) shows protection of the TATAAA box. Individual bands were quantified, and signals from the TBP-TFIIA-bound probe were compared with the unbound probe (Fig. 4C). On the *ADH2* promoter, hypersensitivity was observed immediately upstream of the TATA element (see Fig. 4B and C, black bars). This upstream OP-Cu sensitivity may be similar to upstream DNase I hypersensitivity seen on the adenovirus MLP, which is dependent upon TFIIA binding (3). TBP also showed very weak protection around a region of the *ADH1* promoter 20 bases downstream of the TATA box (see gray bars in Fig. 4C). This region corresponds to a stretch of four thymidines that may constitute a weak TBP-binding site. In general, apart from the protection of the TATA box, there is remarkable similarity between the TBP-TFIIA-bound probe and the unbound probe.

The TFIID-TFIIA complex also showed protection of the TATA box (see Fig. 4, A and B, lanes 2 and 5, and D). In addition, there was increased digestion upstream and especially downstream of the *ADH1* and *ADH2* TATA boxes compared with TBP-TFIIA. These suggest some TAF-dependent contacts or conformation changes. Changes in digestion patterns were seen extending from both upstream and downstream of the TATA box, indicating extensive contacts between TFIID and the promoter. There was a general increase in OP-Cu sensitivity on both strands of the region upstream of the TATA element, extending about 40 bp in each direction. This increased digestion echoes a previous observation of a general increase in DNase I sensitivity seen with yeast TFIID (10).

On the downstream side, both strands of the *ADH1* and *ADH2* promoters showed regions of significantly increased cleavage. On the antisense strands these extended 15 bp from the downstream edge of the TATA element. On the sense strands, three areas of increased sensitivity were seen, with peaks around 7, 18, and 29 bp downstream of the TATA box (Fig. 4D). This 11-bp repeating pattern of the downstream digestion pattern is reminiscent of the DNase I digestion pattern seen with mammalian TFIID (see Fig. 6 in Ref. 30). The periodicity suggests that only one face of the downstream DNA may be in close contact with TFIID. Most interestingly, the peaks of increased TAF-dependent digestion often corresponded to short stretches of thymidines.

Cross-linking of TFIID to the *ADH1* Promoter—As a complement to the footprint experiments, we used an oligonucleotide-based approach to synthesize nine probes with a photoreactive cross-linker substituted for thymidine at different sites within the promoter region. Upon activation with UV light, an aryl azido group covalently links to proteins within a radius of ~1 nm. Following DNA digestion, proteins in sufficiently close proximity to the major groove were left with a small covalently attached radiolabel. These proteins were resolved by SDS-PAGE, and the radiolabels were detected with a PhosphorImager. We used this method to analyze the binding of TFIID to a modified yeast *ADH1* promoter in conjunction with TFIIA (Fig. 5). Tentative TAF assignments were based on molecular weight and comparison with specific immunoblots of purified TFIID.

As expected from the footprinting experiments, TAF cross-linking was seen at least 30 bp upstream and downstream of the TATA box. Although some of this cross-linking is undoubtedly background signal, specific cross-linking enrichments were seen throughout the sense strand of the promoter. Bands that probably represent Taf11 and HCHH-Taf13 cross-link

most strongly immediately downstream of where TBP binds to the TATA element minor groove. Taf2 cross-linking was seen from -25 to +12 but not further downstream. Cross-linking of another protein, tentatively identified as Taf14, was also strongest in this upstream region. In contrast, two bands in the range of 130–140 kDa showed strongest cross-linking from +6 to +32. The signal from these two bands always tracked equally, and we believe they represent the two Taf1 species identified in the mass spectroscopy analysis. Similarly, the band corresponding to the expected position of Taf3 and/or Taf4 appears to increase in intensity in this downstream promoter region. These proteins show the strongest cross-linking at positions +12 and +24, whereas Taf1 and Taf5 cross-linking was strongest at +6, +18, and +32. The periodicity seen in our footprints and cross-linking results is consistent with DNase I footprinting experiments of mammalian TFIID that showed alternating protections and hypersensitivities (27, 31).

In Vitro Transcription Activity—TFIID is required for initiation of transcription *in vitro* (32). However, TBP alone is sufficient for basal transcription (33). The mammalian TFIID-extended footprint is altered upon adjacent binding of upstream activators (31). This and other experiments have led to the proposal that TAFs can mediate activated transcription (reviewed in Ref. 34). We tested whether our purified yeast TFIID could mediate basal and activated transcription using an *in vitro* system containing highly purified TFIIB, TFIIE, TFIIIF, TFIIF, and RNA polymerase II but no Mediator complex. Each transcription reaction contains two reporter plasmids. One carries a Gal4-responsive promoter driving a G-less cassette. The second carries a Gcn4-responsive promoter driving a shorter G-less cassette. Under the conditions assayed, transcription was barely supported by TBP alone, and addition of excess TBP did not increase transcription levels. The presence of the TAFs in TFIID improved basal transcription considerably. The ability of the artificial activator Gal4-VP16 to activate transcription in the absence (Fig. 6A, lanes 2 and 3) or presence of the TAFs (lanes 4 and 5) was tested. In reactions supported by TBP, no activation was observed when Gal4-VP16 was added (Fig. 6, lane 3). Adding excess TBP did not alter this result. In the presence of TFIID, a modest but reproducible 2-fold activation was observed. Similar results were observed when Gcn4 was used instead of Gal4-VP16 (data not shown). In all cases, activation was independent of Mediator, because none was present in these reactions.

Because TFIIA stabilizes TFIID binding to DNA, the effect of TFIIA on TFIID-mediated transcription was assayed. The ability of TBP to mediate basal transcription improved by a factor of about 1.2 in the presence of TFIIA (Fig. 6B, lanes 1 and 2). The ability of TFIID to mediate basal transcription improved by a factor of 2 in the presence of TFIIA (Fig. 6B, lanes 3 and 4). We also tested the effect of TFIIA on activated transcription. The addition of Gal4-VP16 activated transcription by a factor of 2 without TFIIA (Fig. 6C, compare lanes 1 and 2). The addition of TFIIA equally increased basal and activated transcription 2-fold (Fig. 6C, lane 3). These effects were independent of the presence of Mediator. When TFIID and Mediator were used together, activated transcription was much stronger than with TFIID alone (data not shown), suggesting that the two co-activators act at different steps in the transcription reaction.

DISCUSSION

Affinity Purification of TFIID—We purified yeast TFIID using a new affinity tag consisting of a CBP motif, two polyhistidine stretches, a TEV protease site, and a triple HA epitope tag. Another group constructed an affinity tag that combined the CBP and polyhistidine tags, but they were unable to use these in combination (35). As with the TAP tag (13), multiple

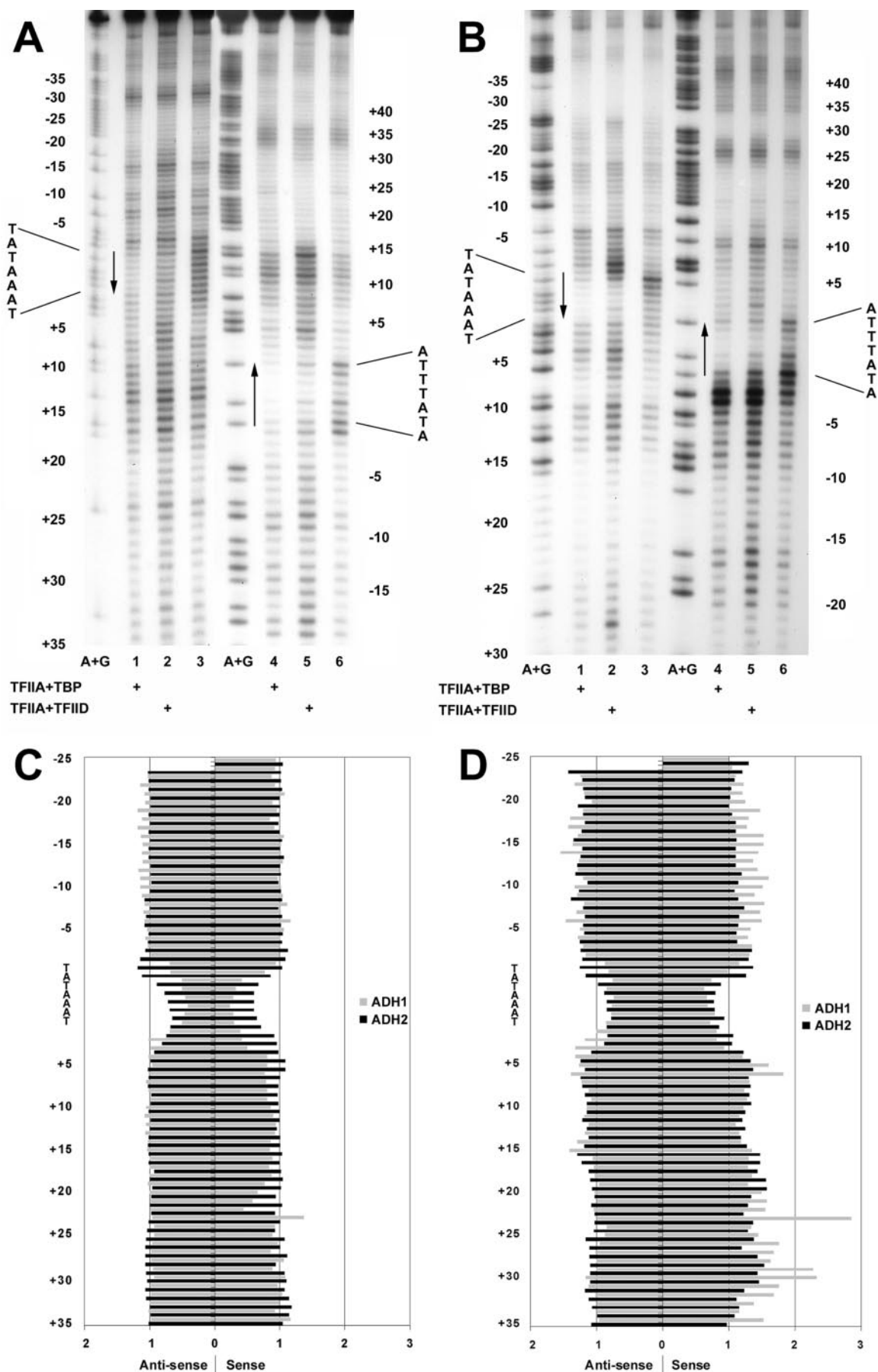


FIG. 4. **TFIIID-TFIIA DNA footprinting.** TFIIA and either TFIIID or recombinant TBP was subjected to analysis by EMSA as in Fig. 3 except that probes contained sequences for the *ADH1* or *ADH2* genes. The gel was then subjected to OP-Cu treatment. Gel slices containing the appropriate protein-DNA complexes were excised, and the DNA was extracted, purified, and analyzed on a urea-8% polyacrylamide sequencing gel.

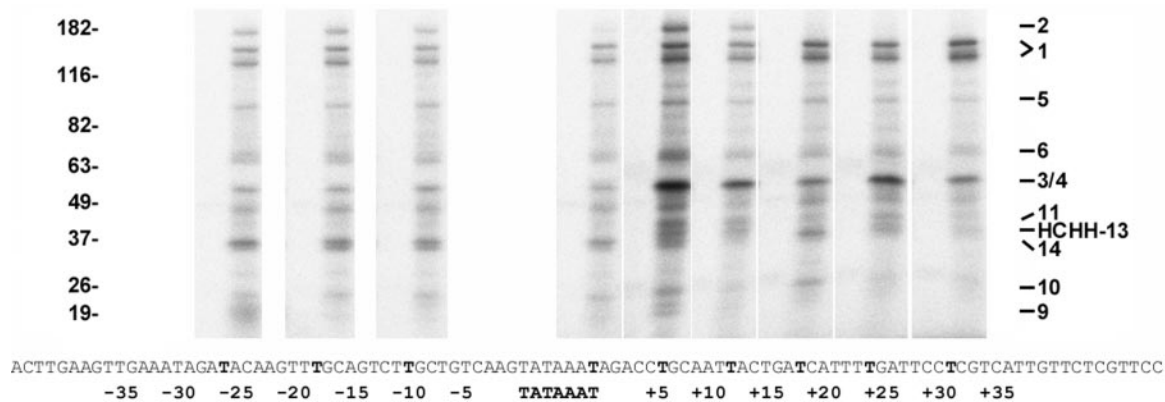


FIG. 5. **Photoaffinity cross-linking of TAFs along the surface of the *ADH1* promoter.** Nine different probes were constructed, each incorporating 5-[*N*-(4-azidobenzoyl)-3-aminoallyl]-dUTP in place of a single thymidine (designated in *boldface*). Binding reactions identical to those used for EMSA experiments were set up for each probe. Following exposure to UV light, enzymatic digestion of DNA, and separation on 4–20% polyacrylamide gels, radioactive proteins were detected by PhosphorImager. In each panel, the *left lane* contains TFIIA alone, and the *right lane* contains TFIID and TFIIA. The panels are arranged by relative position along the sense strand of the *ADH1* promoter. The apparent molecular weights are indicated on the *left* and tentative TAF assignments are on the *right*.

affinity tags make efficient purification possible with a minimum number of chromatography steps. The HCHH tag was designed to be relatively compact at only 118 residues with an apparent molecular mass of 13.7 kDa. The CBP module allows elution with EGTA under mild conditions. Chromatography on immobilized nickel or cobalt columns provides a powerful purification step, although the dual poly-histidine tags require a relatively high concentration of imidazole for elution. The TEV protease site could also be used for elution. Because the buffers for the calmodulin and immobilized metal columns are incompatible, we used a standard ion exchange column to change the buffers and to provide an additional purification step. The presence of the triple HA epitope within the HCHH tag potentially provides an additional affinity purification step but was used here for tracking the tagged Taf13 protein by immunoblotting.

The HCHH purification of TFIID succeeded on several levels. Foremost, our purified TFIID contained all 14 TBP-associated factors that have been identified using completely different methods (1). Significant quantities of TFIID complex were obtained from each preparation. Although we have not done a side-by-side comparison, in our hands the yields of TFIID are better with the HCHH tag than those obtained using standard TAP purification. The HCHH-purified TFIID complex was active in both DNA binding and transcription assays.

Several additional proteins were found in the TFIID preparation. Many were abundant proteins that are common contaminants in many purifications (23). These proteins also appeared in a control purification from untagged yeast extracts. The TFIID preparation also contained Cka1, Cka2, Ubp3, Bre5, Bul1, and Rsp5. Kinase assays and anti-ubiquitin Western blots suggest that these proteins could be involved in regulation of TFIID. This connection is made more likely by previous observations that have implicated them in transcription regulation.

Cka1 and Cka2 are the catalytic subunits of casein kinase II (CK2). CK2 can affect transcription by RNA polymerase II (36) and may directly (37) or indirectly (38) regulate polymerase II

through its C-terminal domain. It has recently been shown that CK2 binds and phosphorylates Bdf1 (26), a protein associated with TFIID (24) and the SWR-C complex (39). It remains to be seen whether there are genuine CK2 phosphorylation sites in any of the TFIID subunits. CK2 has also been implicated in regulation of RNA polymerases I (40, 41) and III (42, 43), suggesting it may be a global regulator of eukaryotic transcription.

Two complexes related to ubiquitination, Ubp3-Bre5 and Rsp5-Bul1, were found in our TFIID preparation. These complexes have both been implicated in transcription. The E3 ligase Rsp5 was initially identified because it “Reverses the SPT-Phenotype”⁴ of an *SPT3* mutation. Spt3 is a component of the TAF-containing SAGA complex (44). Most interestingly, yeast Taf12 (a component of both TFIID and the SAGA complexes) has a predicted binding site for the Rsp5 WW domain (45). Rsp5 may also regulate elongation of transcription (46), perhaps by mediating ubiquitination of stalled RNA polymerase molecules (45). Rsp5 associates with Bul1 as part of a large 40 S protein complex (47). The de-ubiquitinating enzyme Ubp3 associates with Bre5, and both have been shown to have roles in regulating exocytosis (48). Of course, this finding does not preclude other roles. Ubp3 antagonizes transcriptional silencing by the SIR proteins in yeast (49). It has been reported that mammalian Taf1 has ubiquitin ligase activity (50), further supporting a connection between TFIID and ubiquitination. When our TFIID preparation is probed with anti-ubiquitin antibodies, multiple proteins are recognized. We have shown that Taf1 and Taf5 are ubiquitinated and may be among the targets of Ubp3-Bre5 and Rsp5-Bul1 (Fig. 2B). It will be interesting to see whether Ubp3-Bre5 and Rsp5-Bul1 antagonize each to regulate ubiquitination of TFIID or other proteins related to transcription.

DNA Binding and Transcription Activities of TFIID—TFIID

⁴ A. Happel and F. Winston, personal communication.

Chemical digestion was used to obtain a sequence ladder (A+G) for each labeled strand to act as a size marker. For each strand the number of base pairs relative to the edges of the TATA element are indicated. The position and orientation of the TATA box are shown by an *arrow*. *A*, analysis of the *ADH1* promoter. *Lanes 1–3* are the top strand, and *lanes 4–6* are the bottom strand. *Lanes 1* and *4* show patterns from TBP-TFIIA. *Lanes 2* and *5* show bound TFIID-TFIIA. *Lanes 3* and *6* show the digestion pattern of the free probe. *B*, same as in *A*, but analyzing the *ADH2* promoter. *C* and *D*, quantitation of gels shown in *A* and *B*. The bands were quantitated by densitometry, and the ratio of the digestion signals from the bound probe relative to the unbound probe was plotted by position relative to the TATA box. A ratio below 1 indicates protection, whereas a ratio above 1 denotes increased sensitivity. The bars on the *left* (negative) side represent the antisense strand, whereas the sense strand is shown to the *right*. Gray bars represent the *ADH1* promoter, and black bars represent the *ADH2* promoter. *C* shows the TBP-TFIIA complex, and *D* shows the TFIID-TFIIA complex.

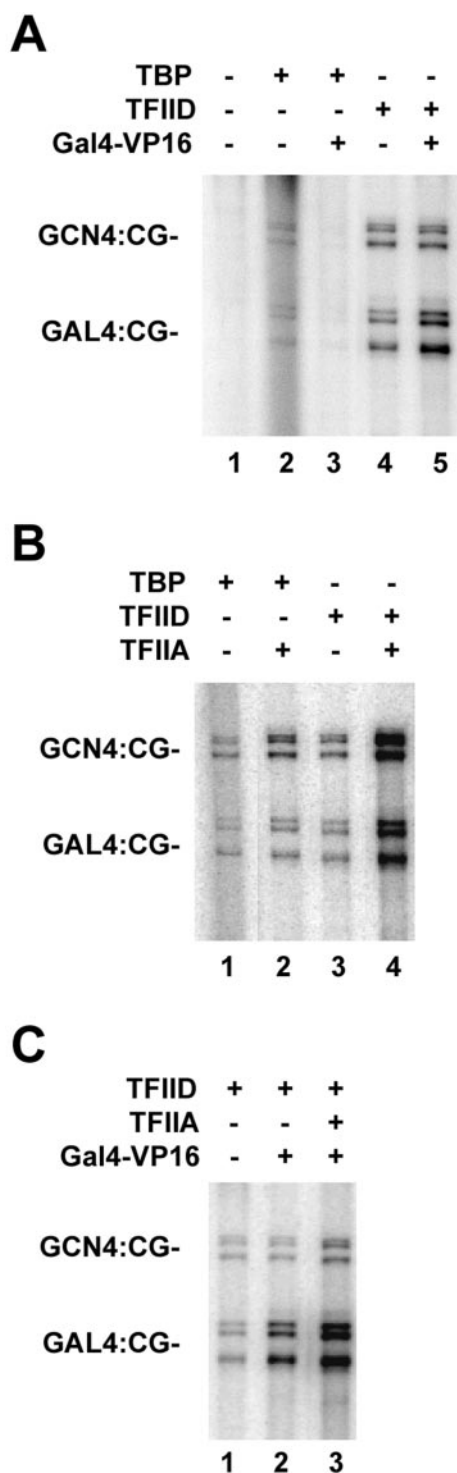


FIG. 6. TFIID supports activated transcription in a Mediator-independent fashion. Reconstituted transcription assays contained purified TFIIB, TFIIE, TFIIF, TFIIH, and RNA polymerase II. TBP (30 ng), an equimolar amount of TFIID (supplemented with TBP such that there is an equimolar amount of TBP to the reactions with TBP alone), TFIIA (15 ng), and Gal4-VP16 (2.5 ng) were added as indicated. RNA products from each of two G-less cassette DNA templates were extracted, precipitated, and subjected to electrophoresis. *A*, response to the GAL4-VP16 activator. No specific transcripts were observed without TBP or TFIID (lane 1). TBP supported basal transcription but did not respond to Gal4-VP16 (compare lanes 2 and 3). TFIID supported basal (lane 4) but transcription of the GAL4:CG-template was also stimulated 2-fold in the presence of Gal4-VP16 (lane 5). *B*, TFIIA stimulates transcription supported by TBP or TFIID. TFIIA was added (lanes 2 and 4) to reactions supported by either TBP (lanes 1 and 2) or TFIID (lanes 3 and 4). *C*, TFIIA stimulates both activated and basal transcription. The indicated factors were added, and transcription was

purified using the HCHH tag contained TBP and was active in both DNA binding and *in vitro* transcription assays. By using native agarose gel electrophoresis, we were able to observe the TFIID-DNA complex, although this complex was greatly stabilized by TFIIA. Similar strong stabilization is seen by DNase I footprinting (10). Most interestingly, the yeast TFIID retarded the probe mobility to a much greater extent than TBP alone. This contrasts with gel shifts of mammalian TFIID-TFIIA, which were reported to have a mobility indistinguishable from that of TBP-TFIIA (51).

The OP-Cu digestion patterns of the *ADH1* and *ADH2* promoters are quite similar despite the fact that they have been classified as "TFIID-independent" and "TFIID-dependent," respectively (52, 53). Indeed, the only major difference appears to be immediately upstream of the TATA box, where *ADH2* has strong hypersensitivity that is not seen on *ADH1*. This hypersensitivity is most obvious with TFIID but is also seen with TBP. The difference between the two promoters may simply reflect sequence differences or different interactions with TFIIA, which is known to bind in this region.

We used OP-Cu to footprint the TFIID-TFIIA-DNA complex, and we found that the interaction pattern with this reagent is in very good agreement with DNase I protection patterns of the same complex (Fig. 4). Very clear protection of the TATA box is observed. There is evidence for TFIID interactions as far as 40 bp upstream of the TATA box to 40 bp downstream. In some areas protection is seen, but more often there is a significant increase in digestion. Sanders *et al.* (10) also noted significant increases in DNase I digestion both upstream and downstream of the TATA boxes with the yeast TFIID-TFIIA complex. The OP-Cu cutting pattern suggests a clear orientation to TFIID binding because the upstream digestion pattern is very different from the downstream one. The downstream interactions show a repeating pattern of increased sensitivities that is reminiscent of mammalian TFIID DNase I footprinting patterns (30). A similar periodicity of cross-linking for some TAFs is seen in that region (Fig. 5). Thus it seems likely that several of the TAFs lie along a particular face of the DNA.

Insights into TFIID structure have come from cross-linking studies placing individual TAFs along the promoter (7, 8, 54) and from immunolocalization studies that place the TAFs within a low resolution electron micrograph structure (11, 55). Both yeast and mammalian TFIID appear as a tri-lobed structure. A central lobe C containing Taf4, Taf10, TBP, and the N-terminal region of Taf1 is flanked by globular domains A and B. Two molecules of Taf5 appear to link the domains together. Both A and B contain the histone-like TAFs, whereas lobe A also contains Taf7 and the bulk of Taf1 (12). Based on our results and those of others, a model can be proposed in which lobes A and B lie along the DNA, one upstream and one downstream of TBP bound to the TATA box. We speculate that lobes B and C, which probably contain TAF2, interact primarily with DNA upstream of the TATA box.

As expected for a fully functional complex, the HCHH-purified TFIID supported both basal and activated transcription (Fig. 6). TFIIA improves transcription with TFIID, presumably by enhancing TFIID binding to DNA (Fig. 2). Most interestingly, TAF-dependent activation of transcription by Gal4-VP16 occurred in the absence of Mediator. However, the addition of Mediator led to higher levels of activation, consistent with suggestions that TFIID and Mediator act at different steps of transcription (56).

quantified. TFIIA stimulated basal transcription 2-fold (comparing the GCN4:CG-template in lanes 2 and 3). TFIIA also stimulated activated transcription 2-fold (comparing the GAL4:CG-template in lanes 2 and 3).

Acknowledgments—We thank S. Tan for recombinant transcription factors; J. Reese and P. A. Weil for anti-TAF antibodies and other reagents; S. Hahn for FLAG-Taf constructs; and J. Workman for Tra1 reagents. We also thank J. Tanny for helpful discussions and the HMS Taplin Mass Spectrometry Facility for assistance.

REFERENCES

- Sanders, S. L., Jennings, J., Canutescu, A., Link, A. J., and Weil, P. A. (2002) *Mol. Cell Biol.* **22**, 4723–4738
- Tora, L. (2002) *Genes Dev.* **16**, 673–675
- Buratowski, S., Hahn, S., Guarente, L., and Sharp, P. A. (1989) *Cell* **56**, 549–561
- Bleichenbacher, M., Tan, S., and Richmond, T. J. (2003) *J. Mol. Biol.* **332**, 783–793
- Geiger, J. H., Hahn, S., Lee, S., and Sigler, P. B. (1996) *Science* **272**, 830–836
- Tan, S., Hunziker, Y., Sargent, D. F., and Richmond, T. J. (1996) *Nature* **381**, 127–151
- Oelgeschlager, T., Chiang, C. M., and Roeder, R. G. (1996) *Nature* **382**, 735–738
- Chalkley, G. E., and Verrijzer, C. P. (1999) *EMBO J.* **18**, 4835–4845
- Burke, T. W., and Kadonaga, J. T. (1996) *Genes Dev.* **10**, 711–724
- Sanders, S. L., Garbett, K. A., and Weil, P. A. (2002) *Mol. Cell Biol.* **22**, 6000–6013
- Leurent, C., Sanders, S., Ruhlmann, C., Mallouh, V., Weil, P. A., Kirschner, D. B., Tora, L., and Schultz, P. (2002) *EMBO J.* **21**, 3424–3433
- Leurent, C., Sanders, S. L., Demeny, M. A., Garbett, K. A., Ruhlmann, C., Weil, P. A., Tora, L., and Schultz, P. (2004) *EMBO J.* **23**, 719–727
- Rigaut, G., Shevchenko, A., Rutz, B., Wilm, M., Mann, M., and Seraphin, B. (1999) *Nat. Biotechnol.* **17**, 1030–1032
- Buratowski, S., Hahn, S., Sharp, P. A., and Guarente, L. (1988) *Nature* **334**, 37–42
- Kuwabara, M. D., and Sigman, D. S. (1987) *Biochemistry* **26**, 7234–7238
- Sengupta, S. M., Persinger, J., Bartholomew, B., and Peterson, C. L. (1999) *Methods* **19**, 434–446
- Bartholomew, B., Kassavetis, G. A., and Geiduschek, E. P. (1991) *Mol. Cell Biol.* **11**, 5181–5189
- Myers, L. C., Leuther, K., Bushnell, D. A., Gustafsson, C. M., and Kornberg, R. D. (1997) *Methods* **12**, 212–216
- Henry, N. L., Sayre, M. H., and Kornberg, R. D. (1992) *J. Biol. Chem.* **267**, 23388–23392
- Kim, Y. J., Bjorklund, S., Li, Y., Sayre, M. H., and Kornberg, R. D. (1994) *Cell* **77**, 599–608
- Lee, T. I., and Young, R. A. (1998) *Genes Dev.* **12**, 1398–1408
- Simos, G., Segref, A., Fasiolo, F., Hellmuth, K., Shevchenko, A., Mann, M., and Hurt, E. C. (1996) *EMBO J.* **15**, 5437–5448
- Gavin, A. C., Bosche, M., Krause, R., Grandi, P., Marzioch, M., Bauer, A., Schultz, J., Rick, J. M., Michon, A. M., Cruciat, C. M., Remor, M., Hofert, C., Schelder, M., Brajenovic, M., Ruffner, H., Merino, A., Klein, K., Hudak, M., Dickson, D., Rudi, T., Gnau, V., Bauch, A., Bastuck, S., Huhse, B., Leutwein, C., Heurtier, M. A., Copley, R. R., Edelmann, A., Querfurth, E., Rybin, V., Drewes, G., Raida, M., Bouwmeester, T., Bork, P., Seraphin, B., Kuster, B., Neubauer, G., and Superti-Furga, G. (2002) *Nature* **415**, 141–147
- Matangkasombut, O., Buratowski, R. M., Swilling, N. W., and Buratowski, S. (2000) *Genes Dev.* **14**, 951–962
- Ranish, J. A., Yi, E. C., Leslie, D. M., Purvine, S. O., Goodlett, D. R., Eng, J., and Aebersold, R. (2003) *Nat. Genet.* **33**, 349–355
- Sawa, C., Nede, E., Krogan, N., Wada, T., Handa, H., Greenblatt, J., and Buratowski, S. (2004) *Mol. Cell Biol.* **24**, 4734–4742
- Sawadogo, M., and Roeder, R. G. (1985) *Cell* **43**, 165–175
- Nakajima, N., Horikoshi, M., and Roeder, R. G. (1988) *Mol. Cell Biol.* **8**, 4028–4040
- Kuwabara, M., Yoon, C., Goyno, T., Thederahn, T., and Sigman, D. S. (1986) *Biochemistry* **25**, 7401–7408
- Emami, K. H., Jain, A., and Smale, S. T. (1997) *Genes Dev.* **11**, 3007–3019
- Horikoshi, M., Carey, M. F., Kakidani, H., and Roeder, R. G. (1988) *Cell* **54**, 665–669
- Sawadogo, M., and Roeder, R. G. (1985) *Proc. Natl. Acad. Sci. U. S. A.* **82**, 4394–4398
- Sayre, M. H., Tschochner, H., and Kornberg, R. D. (1992) *J. Biol. Chem.* **267**, 23376–23382
- Burley, S. K., and Roeder, R. G. (1996) *Annu. Rev. Biochem.* **65**, 769–799
- Honey, S., Schneider, B. L., Schieltz, D. M., Yates, J. R., and Futcher, B. (2001) *Nucleic Acids Res.* **29**, E24
- Dahmus, M. E. (1981) *J. Biol. Chem.* **256**, 3332–3339
- Chapman, R. D., Palancade, B., Lang, A., Bensaude, O., and Eick, D. (2004) *Nucleic Acids Res.* **32**, 35–44
- Palancade, B., Dubois, M. F., and Bensaude, O. (2002) *J. Biol. Chem.* **277**, 36061–36067
- Krogan, N. J., Keogh, M. C., Datta, N., Sawa, C., Ryan, O. W., Ding, H., Haw, R. A., Pootoolal, J., Tong, A., Canadien, V., Richards, D. P., Wu, X., Emili, A., Hughes, T. R., Buratowski, S., and Greenblatt, J. F. (2003) *Mol. Cell* **12**, 1565–1576
- Saez-Vasquez, J., Meissner, M., and Pikaard, C. S. (2001) *Plant Mol. Biol.* **47**, 449–459
- Hannan, R. D., Hempel, W. M., Cavanaugh, A., Arino, T., Dimitrov, S. I., Moss, T., and Rothblum, L. (1998) *J. Biol. Chem.* **273**, 1257–1267
- Johnston, I. M., Allison, S. J., Morton, J. P., Schramm, L., Scott, P. H., and White, R. J. (2002) *Mol. Cell Biol.* **22**, 3757–3768
- Hu, P., Wu, S., and Hernandez, N. (2003) *Mol. Cell* **12**, 699–709
- Grant, P. A., Duggan, L., Cote, J., Roberts, S. M., Brownell, J. E., Candau, R., Ohba, R., Owen-Hughes, T., Allis, C. D., Winston, F., Berger, S. L., and Workman, J. L. (1997) *Genes Dev.* **11**, 1640–1650
- Chang, A., Cheang, S., Espanel, X., and Sudol, M. (2000) *J. Biol. Chem.* **275**, 20562–20571
- Wu, X., Chang, A., Sudol, M., and Hanes, S. D. (2001) *Curr. Genet.* **40**, 234–242
- Yashiroda, H., Oguchi, T., Yasuda, Y., Toh, E. A., and Kikuchi, Y. (1996) *Mol. Cell Biol.* **16**, 3255–3263
- Cohen, M., Stutz, F., Belgareh, N., Haguenaer-Tsapis, R., and Dargemont, C. (2003) *Nat. Cell Biol.* **5**, 661–667
- Moazed, D., and Johnson, D. (1996) *Cell* **86**, 667–677
- Pham, A. D., and Sauer, F. (2000) *Science* **289**, 2357–2360
- Lieberman, P. M., and Berk, A. J. (1991) *Genes Dev.* **5**, 2441–2454
- Kuras, L., Kosa, P., Mencia, M., and Struhl, K. (2000) *Science* **288**, 1244–1248
- Komarnitsky, P. B., Klebanow, E. R., Weil, P. A., and Denis, C. L. (1998) *Mol. Cell Biol.* **18**, 5861–5867
- Burke, T. W., and Kadonaga, J. T. (1997) *Genes Dev.* **11**, 3020–3031
- Andel, F., III, Ladurner, A. G., Inouye, C., Tjian, R., and Nogales, E. (1999) *Science* **286**, 2153–2156
- Wu, S. Y., Zhou, T., and Chiang, C. M. (2003) *Mol. Cell Biol.* **23**, 6229–6242